The simplest discrete Radon transform

Peter W. Cary, Sensor Geophysical Ltd.

Summary

Pitfalls in the evaluation of the discrete Radon transform are reviewed and methods are identified that overcome the problems. A commonly used discrete form of the Radon integral formula results in two types of artifacts being generated: operator aliasing artifacts and truncation artifacts. Operator aliasing artifacts can be avoided by taking into account the bandlimited nature of the integrand during the conversion of the Radon integral into a discrete summation. Truncation artifacts are due to aperture limitation of the input data (missing offsets) and can be overcome by imposing a minimum entropy constraint in model space that forces the solution to be as simple as possible. Eliminating these two types of artifacts produces a clean, simple, and more highly resolved image in the Radon domain for any application such as multiple elimination, predictive deconvolution or migration.

Introduction

When computing the Radon transform of the simple (x,t) domain synthetic data in Figure 1a, aliasing and truncation artifacts such as those in Figure 1b, are easily and commonly generated in the Radon domain, and are sometimes referred to as pitfalls of the discrete Radon transform (Marfurt et al., 1996). The artifacts can be generated not only in images produced by time-invariant forms of the Radon transform (linear, parabolic and hyperbolic), but also in generalized, time- and space-variant Radon transforms, such as Kirchhoff migration. The elimination of operator aliasing artifacts is a relatively straightforward and well-understood problem, but truncation artifacts pose a more difficult problem. Truncation artifacts are a visible reminder of the limit to the attainable resolution of an image that is possible with a given acquisition geometry (Beylkin et al., 1985). Performing a Radon transform to obtain resolution beyond these limits is an ill-posed inverse problem, comparable in form to sparse spike inversion (e.g. Oldenburg et al., 1983), and therefore can only be performed by adding *a priori* information.

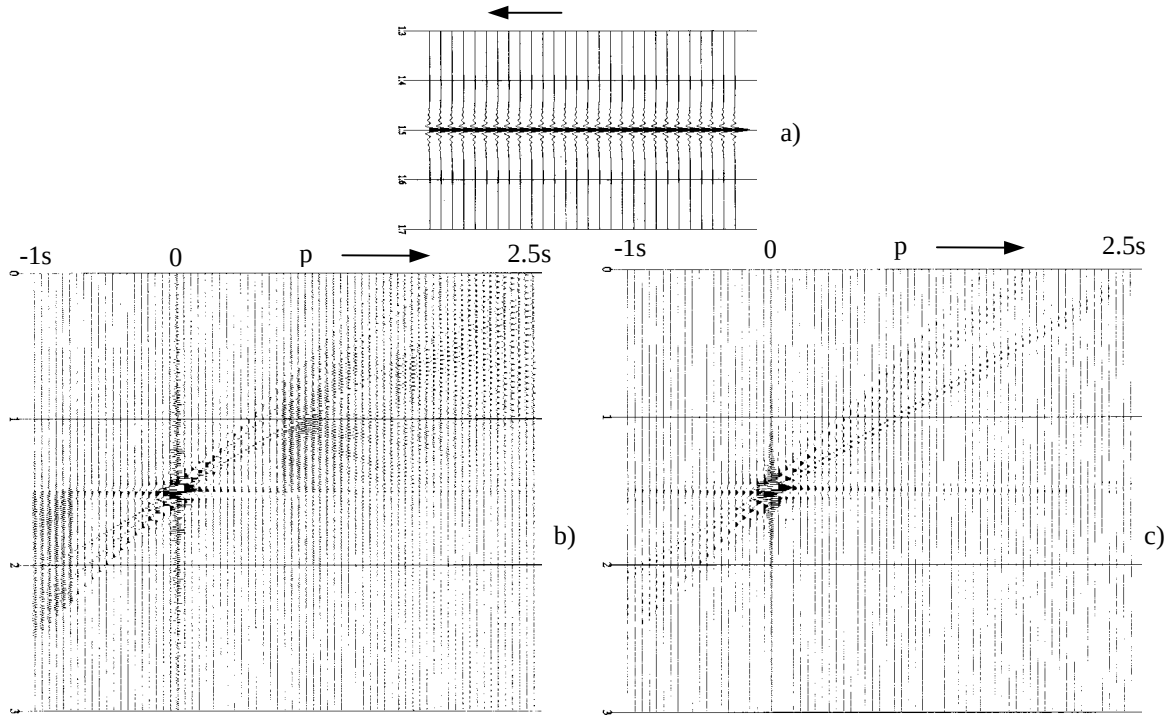

Figure 1 a) Single flat event with 5/10 – 80/100 Hz wavelet. b) Linear Radon transform of a) with operator aliasing and truncation artifacts. c) same as b), but without aliasing artifacts.

Eliminating operator aliasing artifacts

Ad hoc methods such as semblance-weighting (Stoffa et al., 1981) can be used to reduce the amplitude of the artifacts in Radon transforms, but these types of methods produce results of questionable reliability. Hale (1984) realized that the aliasing artifacts are due to operator aliasing, and that they can be eliminated by taking the bandlimited nature of the integrand into account when converting the Radon transform integral equation into a summation, as the following derivation shows. Singh et al. (1989) pointed out the flexibility with which antialiasing conditions can be applied. The same problem has been addressed by Gray (1992) and Lumley et al. (1994) in the context of Kirchhoff migration.

In a simplified form, 2-D Radon transforms are all of the form

$$U(\tau, p) = \iint u(t,x)\delta(t - t'(\tau, p, x))dtdx,$$

where, for example, $t' = \tau + px$ for slant stacks and $t' = (\tau^2 + 4(p-x)^2 / v^2)^{1/2}$ for poststack migration. Aliasing artifacts from steep summation operators are generated when the following commonly used approximation to the Radon integral is used:

$$U(\tau, p) = \sum_l \sum_j u(j\Delta t, l\Delta x) Sinc(\tfrac{t'}{\Delta t} - j), \qquad (1)$$

where $Sinc(x) = \sin(\pi x / \pi x)$. Hale (1984) derived a better approximation to the Radon integral by assuming that u(t,x) is bandlimited in both time and space, with Δt and Δx defining the Nyquist sample rates. In this case, the continuous wavefield, u(t,x), can be exactly reconstructed from its discrete samples with sinc function interpolation:

$$u(t,x) = \sum_l \sum_j u(j\Delta t, l\Delta x) Sinc(\tfrac{t}{\Delta t} - j) Sinc(\tfrac{x}{\Delta x} - l).$$

Substituting this expression into the Radon integral, taking the summations outside the integral, and carrying out an approximate evaluation of the remaining integral, we get:

$$U(\tau, p) = \sum_l \sum_j u(j\Delta t, l\Delta x) q(l\Delta x) Sinc\{q(l\Delta x)(\tfrac{t'}{\Delta t} - j)\}, \qquad (2)$$

where $q(l\Delta x) = \min(1, \frac{\Delta t}{\Delta x}\left|\frac{dt'}{dx}\right|^{-1})$. The only assumption used to evaluate the integral over x is that the line of integration curves slowly enough that $t'(x) \cong t'(l\Delta x) + (x - l\Delta x)\frac{dt'}{dx}$. The $q(l\Delta x)$ factors in the final summation antialias the summation operator by filtering the aliased frequencies from the interpolating sinc function. Using this equation, operator aliasing artifacts can be eliminated from the Radon image as long as the input data is not aliased with respect to the data along the Radon summation trajectories, and as long as the summation trajectory is relatively linear within the effective width of the interpolating sinc function. Fig. 1b was calculated with (1), and Fig. 1c was calculated with (2). With due care to the sampling of the input data, these assumptions can usually be satisfied for most forms of Radon transform. An exception to the latter assumption is DMO at late times because of the operator's large curvature.

Eliminating truncation artifacts

The truncation artifacts that remain in Figure 1c result from gaps in the input data and missing data at near and far offsets. An ad hoc method for reducing the amplitude of these artifacts is to taper the amplitudes of the input data at the edges. However, this produces a transformed result that is inconsistent with the original data, and therefore does not really solve the problem, especially if the near offsets are crucial to the problem, as in multiple attenuation. The nonuniqueness of the Radon transform resulting from missing data was first investigated by Thorson and Claerbout (1985), who used a time-domain algorithm that attenuated truncation artifacts with a nonlinear sparseness constraint. Their time-variant hyperbolic transform was expensive to compute, and consequently was abandoned once Hampson's (1986) fast, time-invariant parabolic transform was introduced. Nevertheless, Hampson's fast, least-squares solution suffers from truncation artifacts. To overcome this problem, Sacchi and Ulrych (1995) introduced a frequency-domain sparseness algorithm that constrains the solution in the p direction, and is relatively fast. Unfortunately, sparseness in the p direction is a necessary, but insufficient, condition for a desirable solution, as the following example shows, so a constraint that is more expensive to impose, such as the one proposed by Thorson and Claerbout, appears to be required in most cases.

Consider the three bandlimited, constant amplitude parabolas in Figure 2a, with moveout at the far offset of –10, 0 and 10 ms respectively. Since these data satisfy the assumed constant-amplitude parabolic model of the transform exactly, we would expect that the Radon transform of Figure 2a would be three separate bandlimited wavelets at p = -10, 0 and 10 ms respectively, as shown in Figure 2e. However, instead of obtaining this desired, simple solution, the standard least-squares solution yields the complex solution in Figure 2b. Taken at face value, the solution in Figure 2b would lead us to believe that each parabola in

Figure 2a is in fact not a single parabola, but is instead a superposition of a number of parabolas of different moveout, wavelet shape and amplitude. This example illustrates the nonuniqueness in the solution of the limited-aperture Radon transform. Many different Radon solutions are able to explain the data in Figure 2a. Figures 2b, c, d and e are four of them. How are we to know which of these is the "right" solution? Based only on their ability to predict the data in a least-squares sense, there is essentially no way to distinguish between them because their inverse transforms (Fig. 2f to 2i) are basically the same, within small error.

Given the choice between simple and complex solutions to a problem, it is best to choose the simplest solution, i.e. the model that is able to explain the data with the smallest number of events in the Radon domain. All four solutions in Figure 2 were obtained by minimizing an objective function of the form, $\phi = \mathbf{e}^{\mathbf{T}}\mathbf{e} + \lambda S(\mathbf{m})$. The first term is the squared-error constraint on the data and the second term is the model constraint. Figure 2b used $S(m_i) = \sum_j m_{ij}^2$ (i is the frequency index and j is the p index), which ensures stability of the inversion by constraining the overall size of the model. Figure 2c is one solution obtained with the nonlinear sparseness algorithm of Sacchi and Ulrych (1995), which uses a frequency-domain algorithm with a minimum entropy model constraint in the p direction: $S(m_i) = \sum_j \ln(m_{ij}^2 + b)$, where b is a small constant. Figure 2d used the same type of constraint in both the τ and p direction in a time-domain algorithm: $S(m) = \sum_i \sum_j (m_{ij}^2 + b)$, which is essentially the algorithm suggested by Thorson and Claerbout (1985). In all cases constraints were measured over the limited frequency band of the data.

Figure 2c indicates a problem with imposing a sparseness constraint only in the p direction. This particular model satisfies the constraint that the solution be sparse in p since only three nonzero p-values are needed to model the data, but there is obviously an unresolved nonuniqueness in the τ direction. This nonuniqueness is removed by imposing sparseness in the τ and p directions, as illustrated by Figure 2d. Fig. 2d must surely be the simplest possible model that can explain the data since it consists of only three nonzero samples. In fact this model is unnecessarily sparse since it resolves frequencies beyond the bandlimits of the data. However, the desired solution, Figure 2e, is obtained by simply bandpass filtering the model in Figure 2d.

This simple example has shown that sparseness in the p direction is a necessary, but insufficient, condition for a desirable solution, whereas sparseness in the τ and p directions is a sufficient, but unnecessarily restrictive, condition for a desirable solution. In practice, imposing a constraint in the p direction is useful when events are widely separated in the Radon domain, but results becomes very sensitive to parameter selection when attempting to resolve closely spaced events. Although imposing a constraint in the τ and p directions requires a slower, time-domain algorithm, the results are much more predictable, and much less sensitive to parameter selection.

Figure 3 shows a comparison of the standard and sparse Radon transforms on real data. The sparse solution for real data rarely collapses reflections to individual p-values because real data do not fit the parabolic or hyperbolic model exactly. Usually, deviations in traveltime away from the assumed shape of the model cause more spreading of energy than variations in amplitude along the reflections. Nevertheless the separation of the multiple from the primary events is obviously better in the sparse solution, and can lead to improved attenuation. (Hunt et al., 1996).

Acknowledgements

I would like to thank PanCanadian Petroleum Ltd. for encouragement to pursue this work and permission to use the data.

References

Beylkin, G. Oristaglio, M. and Miller, D., 1985, Spatial resolution of migration algorithms: in Proc. 14th Int. Symp. Acoust. Imag., 155-167.
Gray, S.H., 1992, Frequency-selective design of the Kirchhoff migration operator: Geophysical Prospecting, **40**, 565-571.
Hale, D., 1984, personal communication.
Hampson, D., 1986, Inverse velocity stacking for multiple elimination: J. Can. SEG, **22**, 44-55.
Hunt, L., Cary, P. , Upham, W., 1996, The impact of an improved Radon transform on multiple attenuation,SEG Extended Abstracts, 1535-1538.
Lumley, D., Claerbout, J.F. and Bevc, D., 1994, Anti-aliased Kirchhoff 3-D migration, SEG Extended Abstracts, 1282-1285.
Marfurt, K.J., Schneider, R.J., and Mueller, M.C., 1996, Pitfalls of using conventional and discrete Radon transfoms on poorly sampled data: Geophysics, **61**, 1467-1482.
Oldenburg, D.W., Scheuer, T., Levy, S., 1983, Recovery of the acoustic impedance from reflection seismograms: Geophysics, **48**, 1318-1337.
Sacchi, M.D. and Ulrych, T.J., 1995, High resolution velocity gathers and offset-space reconstruction: Geophysics, **60**, 1169-1177.

Singh, S.C., West, G.F., and Chapman, C.H., 1989, On plane-wave decomposition:alias removal: Geophysics, **54**, 1339-1343.
Thorson, J.R. and Claerbout, J.F., 1985, Velocity-stack and slant-stack stochastic inversion: Geophysics, **50**, 2727-2741.

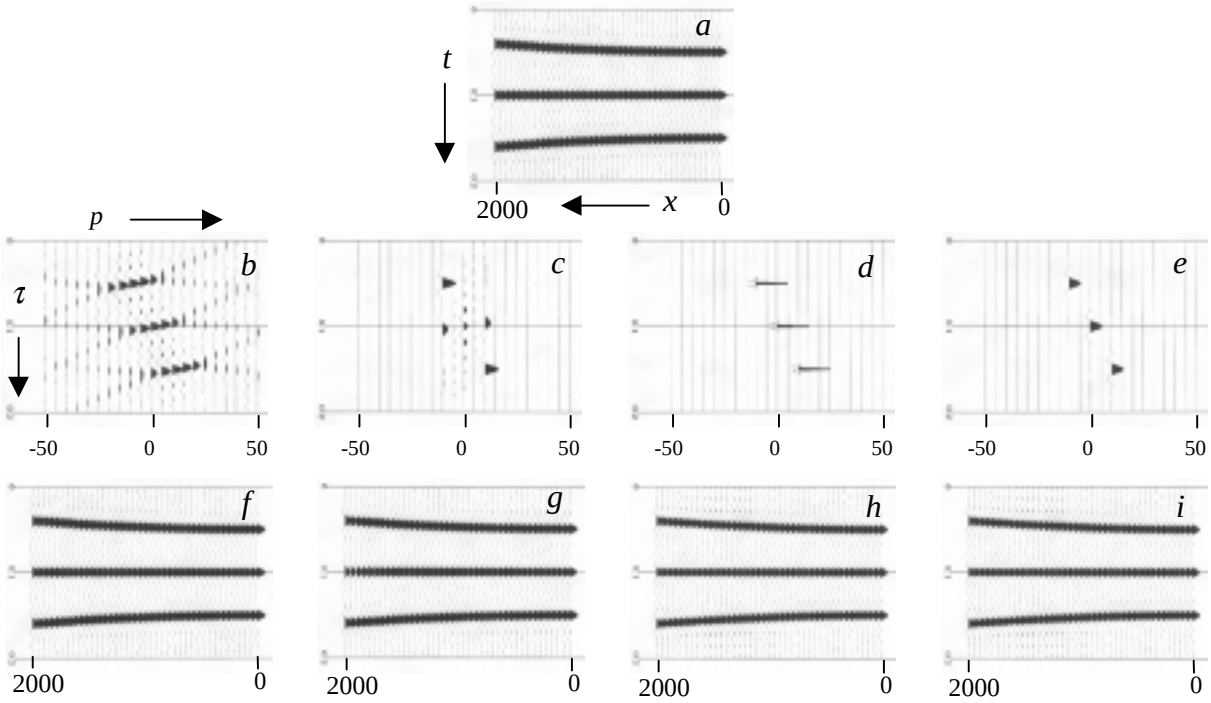

Figure 2 a) Input data. b) standard least-squares Radon transform. c) sparse Radon transform obtained with p-sparseness constraint. d) sparse Radon transform obtained with tau and p-sparseness constraint. e) Same as d) but bandpass filtered to frequency range of input data. f) to i) are inverse Radon transforms of b) to e).

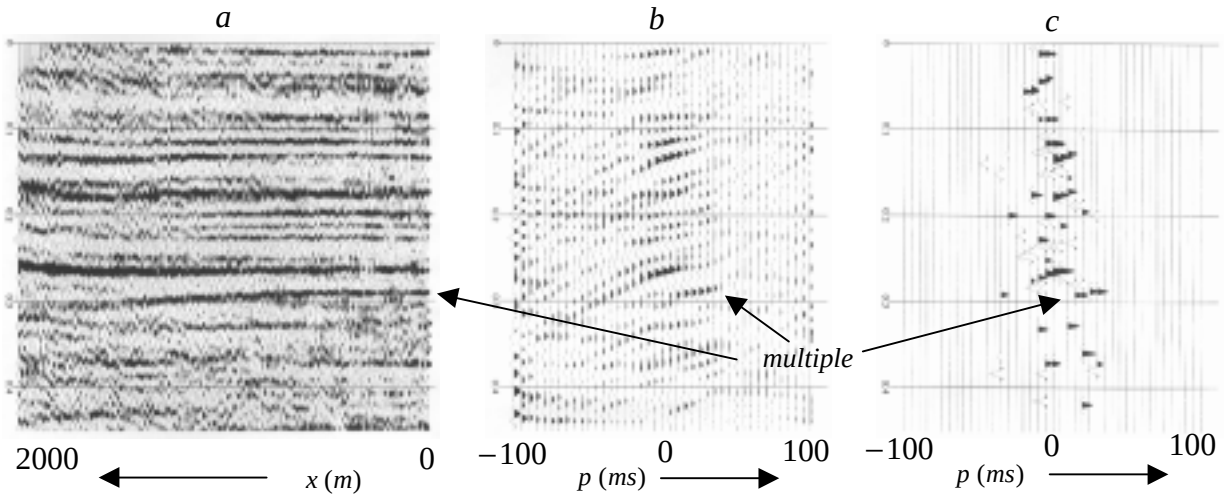

Figure 3 a) Input data. b) Standard least-squares Radon transform c) sparse Radon transform with tau and p constraint